Inorg. Chem. **2003**, *42*, 3662–3669

^{1}H NMR Studies of Ligand and H/D Exchange Reactions of *cis*- and *trans*-([14]aneN$_4$)(H$_2$O)RhH^{2+} in Aqueous Solutions

Kelemu Lemma,[†,‡] Arkady Ellern,[‡] and Andreja Bakac*[,†]

Ames Laboratory and the Department of Chemistry, Iowa State University, Ames, Iowa 50011

Received February 5, 2003

Substitution and exchange reactions of *cis*- and *trans*-L^1(H$_2$O)RhH^{2+} (L^1 = 1,4,8,11-tetraazacyclotetradecane = [14]aneN$_4$) were studied in aqueous solutions by UV–vis and ^{1}H NMR spectroscopies. At pH 1 and 25 °C, the substitution of SCN$^-$ for the coordinated molecule of water is rapid and thermodynamically favorable. Spectrophotometric determinations yielded the equilibrium constants $K = 1.49 \times 10^3$ M^{-1} (cis) and 1.44×10^3 (trans). ^{1}H NMR studies in D$_2$O revealed a rapid dynamic process, interpreted as the exchange between coordinated water and X$^-$ (X = Cl, Br, or I). On the other hand, no line broadening was observed for the strongly bound ligands CN$^-$ and SCN$^-$. The complex *trans*-L^1(D$_2$O)RhH^{2+} undergoes a base-catalyzed H/D exchange of the hydride in D$_2$O with a rate constant of $(1.45 \pm 0.02) \times 10^3$ M^{-1} s^{-1}. The exchange in the cis isomer is very slow under similar conditions. The complex *cis*-[L^{1}ClRhH](ClO$_4$) crystallizes in the centrosymmetric $P\bar{1}$ space group, unit cell dimensions $a = 8.9805(11)$ Å, $b = 9.1598(11)$ Å, $c = 10.4081(13)$ Å, $\alpha = 81.091(2)°$, $\beta = 81.978(2)°$, $\gamma = 88.850(2)°$. The rhodium atom resides in a slightly distorted octahedral environment consisting of the four N atoms of the cyclam, a stereochemically active hydrogen, and a chlorine atom.

Introduction

As the demand for environmentally friendly catalysis increases, so does the importance of aqueous organometallic chemistry. The growing list of known water-soluble organometallic compounds[1−7] includes some reasonably stable transition metal hydrides such as (C$_5$H$_4$CO$_2$H)(CO)$_3$WH[1] and its derivatives (C$_5$H$_4$CO$_2$H)(CO)$_2$(PMe$_3$)WH and (C$_5$H$_4$CO$_2$H)(CO)$_2$[P(OMe)$_3$]WH. A number of other hydrides are also known.[8−15] Strictly speaking, most of them are not organometallic materials in that they lack a metal−carbon bond, but they exhibit rich chemistry and engage in both stoichiometric and catalytic reactions.

It is widely accepted that electronically saturated transition metal hydrides have a M$^{\delta+}$−H$^{\delta-}$ bond polarity, even when such complexes undergo facile acid dissociation in water.[16] The hydridicity increases with the electron-donating power of other ligands in the complex. Depending on the metal, ligands, and added reactants, the hydrides will act as hydrogen atom, hydride, or proton donors.[2,17−21]

Under the right circumstances and in the presence of isotopically enriched solvent and/or other reagents, such

* Author to whom correspondence should be addressed. E-mail: bakac@ameslab.gov.
† Ames Laboratory.
‡ Chemistry Department.

(1) Shafiq, F.; Szalda, D. J.; Creutz, C.; Bullock, R. M. *Organometallics* **2000**, *19*, 824−833.
(2) Cabelli, D. E.; Shafiq, F.; Creutz, C.; Bullock, R. M. *Organometallics* **2001**, *20*, 3729−3737.
(3) Balzarek, C.; Weakley, T. J. R.; Tyler, D. R. *J. Am. Chem. Soc.* **2000**, *122*, 9427−9434.
(4) Funaioli, T.; Cavazza, C.; Marchetti, F.; Fachinetti, G. *Inorg. Chem.* **1999**, *38*, 3361−3368.
(5) Darensbourg, D. J.; Robertson, J. B.; Larkins, D. L.; Reibenspies, J. H. *Inorg. Chem.* **1999**, *38*, 2473−2481.
(6) Avey, A.; Tenhaeff, S. C.; Weakley, T. J. R.; Tyler, D. R. *Organometallics* **1991**, *10*, 3607−3613.
(7) Joo, F.; Nadasdi, L.; Benyei, A.; Csiba, P.; Katho, A. *NATO ASI Ser., Ser. 3* **1995**, *5*, 23−32.
(8) Pearson, R. G. In *Bonding Energetics in Organometallic Compounds*; Marks, T. J., Ed.; American Chemical Society: Washington, 1990; pp 251−262.
(9) Joo, F.; Kovacs, J.; Benyei, A. C.; Katho, A. *Catal. Today* **1998**, *42*, 441−448.
(10) Pearson, R. G. *Chem. Rev.* **1985**, *85*, 41−49.
(11) Weber, J. H.; Schrauzer, G. N. *J. Am. Chem. Soc.* **1970**, *92*, 726−727.
(12) Pearson, R. G.; Ford, P. C. *Comments Inorg. Chem.* **1982**, *1*, 279−291.
(13) Thomas, K.; Osborn, J. A.; Powell, A. R.; Wilkinson, G. *J. Chem. Soc. A* **1968**, 1801−1806.
(14) Coyle, B. A.; Ibers, J. A. *Inorg. Chem.* **1972**, *11*, 1105−1109.
(15) Hanke, D.; Wieghardt, K.; Nuber, B.; Lu, R.-S.; McMullan, R. K.; Koetzle, T. F.; Bau, R. *Inorg. Chem.* **1993**, *32*, 4300−4305.
(16) Poli, R. In *Recent Advances in Hydride Chemistry*, 1st ed.; Peruzzini, M., Poli, R., Eds.; Elsevier Science B. V.: Amsterdam, 2001; pp 139−188.
(17) Bullock, R. M.; Samsel, E. G. *J. Am. Chem. Soc.* **1990**, *112*, 6886−6898.
(18) Bakac, A.; Guzei, I. A. *Inorg. Chem.* **2000**, *39*, 736−740.
(19) Berning, D. E.; Noll, B. C.; DuBois, D. L. *J. Am. Chem. Soc.* **1999**, *121*, 11432−11447.
(20) Eisenberg, D. C.; Norton, J. R. *Isr. J. Chem.* **1991**, *31*, 55−66.

10.1021/ic034130v CCC: $25.00 © 2003 American Chemical Society
Published on Web 05/09/2003

reactions may lead to the H/D exchange at the metal. For example, some Ir(III) hydrides have been reported[22] to exchange hydrogen with D_2O solvent, and $IrH_2(\eta^1\text{-}SC_5H_4NH)_2(PCy_3)_2$ exchanges H with D_2(g) in CH_2Cl_2 via a η^2-dihydrogen intermediate.[23]

Transition metal hydrides undergo facile ligand substitution at the position(s) trans to the hydride, which is known to exhibit a strong trans effect.[15,24−27] Such substitution reactions have considerable utility in the synthesis of derivatives.

In our recent work we have concentrated on a group of rhodium hydrides consisting of tetraammine,[13,25] pentaammine,[13,25] and macrocyclic[28] compounds. These materials are quite stable in solid state and aqueous solution and have been characterized spectroscopically and chemically, and some of them by X-ray crystal structure analysis.[14,19,28]

The present paper deals with the substitution chemistry of two macrocyclic complexes:[28]

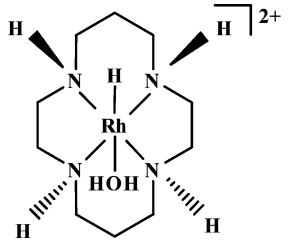

trans-$L^1(H_2O)RhH^{2+}$

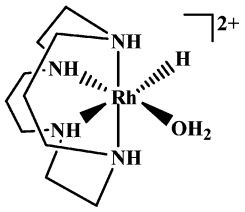

cis-$L^1(H_2O)RhH^{2+}$

They are *trans*-*R*,*R*,*S*,*S*-([14]aneN$_4$)$(H_2O)RhH^{2+}$ and *cis*-*R*,*R*,*R*,*R*-([14]aneN$_4$)$(H_2O)RhH^{2+}$ (hereafter *trans*- and *cis*-$L^1(H_2O)RhH^{2+}$). As described below, both undergo H/D exchange of the rhodium-bound hydrogen. Also, the substitution of coordinated water with Lewis bases was observed. In view of the lability of the coordinated water molecules, the species in D_2O are believed to have the formula $L^1(D_2O)RhH^{2+}$. Some of the equilibrium determinations utilized UV−visible spectroscopy, but most of the work relied on ^{1}H NMR, for which metal hydrides are particularly well suited[29,30] owing to their high-field resonances, well removed from the resonances of most other types of hydrogen atoms present in a typical complex.[31] The hydrogen in rhodium hydrides appears as a doublet owing to the splitting by ^{103}Rh present in 100% abundance.

We also report the results of a single-crystal X-ray crystallographic investigation of *cis*-$[L^1ClRhH](ClO_4)$ to complement our previously reported structure[28] of *trans*-$[L^1ClRhH]_2ZnCl_4$. Although some mononuclear rhodium(III) hydrides have been structurally characterized,[14,32−35] studies of macrocyclic rhodium hydrides are still rare.

Experimental Section

Reagents. Perchlorate salts of *cis*-L^1ClRhH^+ and *trans*-L^1ClRhH^+ were obtained from *cis*- and *trans*-$[L^1ClRhH]_2(ZnCl_4)$, prepared as previously described.[28]

CAUTION! Perchlorate salts are potentially explosive and need to be handled with care. Piperazine-*N*,*N*′-bis(4-butanesulfonic acid, abbreviated as PIPBS (GFS Chemicals), was used to buffer solutions in H/D exchange experiments and in equilibrium measurements at pH 7.6. Dimethyl-d_6 sulfoxide (99.9% D) and acetonitrile-d_3 (99.8% D) (both Cambridge Isotope Laboratories, Inc.) and deuterium oxide (99.9% D, Aldrich) were used as solvents in ^{1}H NMR measurements. All other chemicals were analytical grade or better and were used as received. Deionized water was further purified by passage through a Millipore Milli-Q water purification system. Stock solutions of LiSCN were standardized by titration against silver nitrate using Fe(III) nitrate as indicator.[36] Ionic strength was adjusted with sodium perchlorate.

The pD of D_2O solutions was obtained by adding 0.4 to the value measured with a pH electrode. These pD values and $K_w(D_2O) = 1.54 \times 10^{-15}$ were then used to calculate the concentration of OD^- in Figure 3.

Instrumentation. A Shimadzu 3101 PC spectrophotometer was used for spectral and equilibrium measurements. Proton NMR spectra were obtained by use of a Bruker DRX-400 MHz and a Varian VXR-400 MHz spectrometer. Room temperature chemical shift measurements were made relative to residual ^{1}H resonances of the deuterated solvents used. The weak, but clearly observable signal of the sparingly water-soluble tetramethylsilane, and the intramolecular methylene hydrogens (δ 1.58) of the cyclam ligand were used as markers for low-temperature spectra in D_2O. A Corning ATC pH meter calibrated with pH 7.0 and 10.0 standard buffers (Fisher) was used for pH measurements. Linear and nonlinear least-squares data analysis utilized KaleidaGraph 3.09 PC software.

Equilibrium Measurements. The reactions of *cis*- and *trans*-$L^1(H_2O)RhH^{2+}$ with SCN^- (eq 1) were studied spectrophotometrically at 25.0 (±0.1) °C and pH 1 (both complexes) and pH 7.6 (*trans*-$L^1(H_2O)RhH^{2+}$) in solutions degassed with argon for at least 30 min. Absorbance changes were recorded at the absorption maxima of *cis*-$L^1(H_2O)RhH^{2+}$ and *trans*-$L^1(H_2O)RhH^{2+}$, 284 and 287 nm, respectively. Both complexes reacted rapidly with SCN^-, and equilibrium was attained in mixing time. Solutions of *cis*-$L^1(H_2O)RhH^{2+}$ decompose somewhat more readily (several percent per hour at room temperature and pH 1) than those of the trans

$$\textit{cis}/\textit{trans}\text{-}L^1(H_2O)RhH^{2+} + SCN^- \overset{K}{\rightleftharpoons} \textit{cis}/\textit{trans}\text{-}L^1(SCN)RhH^+ + H_2O \quad (1)$$

(21) Bullock, R. M. *Comments Inorg. Chem.* **1991**, *12*, 1−33.
(22) Paterniti, D. P.; Roman, P. J., Jr.; Atwood, J. D. *Organometallics* **1997**, *16*, 3371−3376.
(23) Lough, A. J.; Park, S.; Ramachandran, R.; Morris, R. H. *J. Am. Chem. Soc.* **1994**, *116*, 8356−8357.
(24) Powell, J.; Shaw, B. L. *J. Chem. Soc. A* **1968**, 617−622.
(25) Osborn, J. A.; Powell, A. R.; Wilkinson, G. *Chem. Commun.* **1966**, 461−462.
(26) Sola, E.; Navarro, J.; Lopez, J. A.; Lahoz, F. J.; Oro, L. A.; Werner, H. *Organometallics* **1999**, *18*, 3534−3546.
(27) Douglas, P. G.; Shaw, B. L. *J. Chem. Soc. A* **1970**, 1556−1557.
(28) Bakac, A.; Thomas, L. M. *Inorg. Chem.* **1996**, *35*, 5880−5884.
(29) Wayland, B. B.; Ba, S.; Sherry, A. E. *J. Am. Chem. Soc.* **1991**, *113*, 5305−5311.
(30) Zhang, X.-X.; Wayland, B. B. *Inorg. Chem.* **2000**, *39*, 5318−5325.
(31) Bakac, A. In *Electron Transfer in Chemistry, Volume 1: Principles, Theories, Methods, and Techniques*; Balzani, V., Ed.; Wiley-VCH: Weinheim, 2001; pp 395−421.
(32) Morales-Morales, D.; Rodriguez-Morales, S.; Dilworth, J. R.; Sousa-Pedrares, A.; Zheng, Y. *Inorg. Chim. Acta* **2002**, *332*, 101−107.
(33) Hughes, R. P.; Kovacik, I.; Lindner, D. C.; Smith, J. M.; Willemsen, S.; Zhang, D.; Guzei, I. A.; Rheingold, A. L. *Organometallics* **2001**, *20*, 3190−3197.
(34) Di Vaira, M.; Rovai, D.; Stoppioni, P.; Peruzzini, M. *J. Organomet. Chem.* **1991**, *420*, 135−142.
(35) Yu, X. Y.; Maekawa, M.; Morita, T.; Chang, H. C.; Kitagawa, S.; Jin, G. X. *Polyhedron* **2002**, *21*, 1613−1620.
(36) Vogel, A. I. *A Textbook of Quantitative Inorganic Analysis*, 4th ed.; Longmans, Green and Co.: New York, 1978.

complex. The precise concentration of each reaction solution was thus determined from the absorbance at 284 nm ($\epsilon = 500$ M^{-1} cm^{-1}) immediately before the injection of thiocyanate.

Kinetics. H/D exchange in *trans*-$L^1(D_2O)RhH^{2+}$ (eq 2) in D_2O was studied in the pD range 7.95−9.12 at 25 °C. Weighed samples

$$\textit{trans}\text{-}L^1(D_2O)RhH^{2+} \xrightarrow{D_2O,\ OD^-} \textit{trans}\text{-}L^1(D_2O)RhD^{2+} \qquad (2)$$

of *trans*-$[L^1(H_2O)RhH](ClO_4)_2$ were placed into a 5-mm NMR tube and gently flushed with argon for 10−15 min. The buffer solution (50 mM, $\mu = 0.1$ M) was prepared by dissolving PIPBS in air-free D_2O containing the appropriate amount of NaOD. One milliliter of this solution was injected into the upper part of the NMR tube. Immediately before the start of data acquisition, the tube was shaken to dissolve the solid. The disappearance of the hydride peak (δ −23.5 ppm) with time was monitored by use of the Bruker spectrometer. Data analysis used XWIN Bruker and KaleidaGraph PC software.

Reactions with Lewis Bases. The interactions between *cis*- and *trans*-$L^1(H_2O)RhH^{2+}$ and I^-, Br^-, Cl^-, CN^-, SCN^-, and acetonitrile were investigated at pH 1 and variable temperature by monitoring the hydride chemical shifts. Proton NMR spectra of air-free solutions of the hydrides (10−20 mM) in D_2O (pD 1) in the presence of added anions (20−100 mM) and/or 10% acetonitrile-d_3 were recorded with use of the Bruker NMR spectrometer. The chemical shifts were measured when constant probe temperature was reached.

Crystallography. Yellow crystals of *cis*-$[L^1ClRhH](ClO_4)$ were obtained by dissolving 50 mg of the complex in air-free water and acidifying the solution to pH 1 with perchloric acid. The solution was concentrated by passing argon over the surface until the crystals began to form. At this point, the stream of argon was discontinued and the solution was kept in the dark for 3 days, during which time the crystals grew to a size convenient for X-ray work. The crystals were isolated and dried in a vacuum desiccator.

A yellow prism with approximate dimensions 0.28 × 0.28 × 0.14 mm^3 was selected under ambient conditions. The crystal was mounted and centered in the X-ray beam with the aid of a video camera. The crystal evaluation and data collection were performed at 298 K with the use of a Bruker CCD-1000 diffractometer (Mo Kα radiation, $\lambda = 0.71073$ Å) and a detector to crystal distance of 5.03 cm.

The initial cell constants were obtained from three series of ω scans at different starting angles. Each series consisted of 30 frames collected at intervals of 0.3° in a 10° range about ω with an exposure time of 5 s per frame. A total of 189 reflections were obtained. The reflections were successfully indexed by an automated indexing routine built in the SMART program. The final cell constants were calculated from a set of 2526 strong reflections from the actual data collection.

The data were collected using the full-sphere routine. A total of 7470 data were harvested by collecting four sets of frames with 0.3° scans in ω with an exposure time of 5 s per frame. This dataset was corrected for Lorentz and polarization effects. The absorption correction was based on fitting a function to the empirical transmission surface as sampled by multiple equivalent measurements[37] using SADABS software. Crystallographic data are reported in Table 1.

Structure Solution and Refinement. The systematic absences in the diffraction data were consistent with the space groups $P1$ and $P\bar{1}$. The *E*-statistics strongly suggested the centrosymmetric space group $P\bar{1}$ and yielded chemically reasonable and computationally stable results of refinement. The position of heavy atom was found by the Patterson method. The remaining atoms were located in an alternating series of least-squares cycles and difference Fourier maps. All non-hydrogen atoms were refined in full-matrix anisotropic approximation. All hydrogen atoms were found objectively on a difference Fourier map and were refined with isotropic displacement coefficients. Final least-squares refinement of 290 parameters against 3749 independent reflections converged to *R* (based on F^2 for $I \geq 2\sigma$) and R_w (based on F^2 for $I \geq 2\sigma$) of 0.028 and 0.073, respectively.

Table 1. Crystallographic Data for *cis*-$[L^1Cl\ RhH](ClO_4)$[a]

empirical formula	$C_{10}H_{25}Cl_2N_4O_4Rh$
fw	439.15
temp	298(2) K
wavelength	0.71073 Å
cryst syst	triclinic
space group	$P\bar{1}$
a	8.9805(11) Å
b	9.1598(11) Å
c	10.4081(13) Å
α	81.091(2)°
β	81.978(2)°
γ	88.850(2)°
V	837.56(18) $Å^3$
Z	2
d(calc)	1.741 Mg/m^3
abs coeff	1.358 mm^{-1}
θ range	2.00−28.27°
index ranges	$-11 \leq h \leq 11$, $-11 \leq k \leq 11$, $-13 \leq l \leq 13$
no. of reflns collcd	7470
no. of indep reflns	3749 ($R_{int} = 0.0175$)
completeness to $\theta = 28.27°$	90.6%
abs correction	empirical
max and min transm	0.72 and 0.56
refinement meth	full-matrix least-squares on F^2
data/restraints/params	3749/0/290
GOF on F^2	1.050
final *R* indices [$I \geq 2\sigma(I)$]	R1[b] = 0.0284, wR2[c] = 0.0734
R indices (all data)	R1[b] = 0.0310, wR2[c] = 0.0754
largest diff peak and hole	0.899 and −0.930 e $Å^{-3}$

[a] L^1 = [14]aneN$_4$. [b] $R1 = \sum||F_o| - |F_c||/\sum|F_o|$. [c] $wR2 = \{\sum[w(F_o^2 - F_c^2)^2]/\sum[w(F_o^2)^2]\}^{1/2}$.

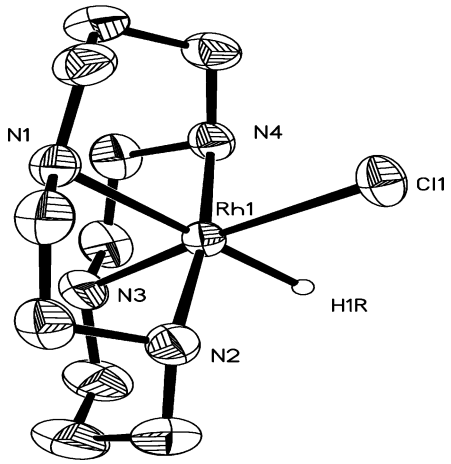

Figure 1. ORTEP drawing of the molecular structure of the cation *cis*-([14]aneN$_4$)$ClRhH^+$. Thermal ellipsoids are drawn at the 50% probability level.

Results and Discussion

Structure of *cis*-$[L^1ClRhH](ClO_4)$. Figure 1 depicts the ORTEP diagram of the cation, *cis*-L^1ClRhH^+. Two mol-

(37) Blessing, R. H. *Acta Crystallogr.* **1995**, *A51*, 33−38.

Table 2. Selected Bond Distances (Å) and Bond Angles (deg) for *cis*-[L^1ClRhH](ClO_4)[a]

Rh(1)−N(3)	2.054(2)	N(3)−Rh(1)−N(2)	92.56(10)
Rh(1)−N(2)	2.069(2)	N(3)−Rh(1)−N(4)	84.42(9)
Rh(1)−N(4)	2.076(2)	N(2)−Rh(1)−N(4)	173.51(9)
Rh(1)−N(1)	2.197(2)	N(3)−Rh(1)−N(1)	97.22(9)
Rh(1)−Cl(1)	2.3784(7)	N(2)−Rh(1)−N(1)	82.89(9)
Cl(2)−O(4)	1.368(4)	N(4)−Rh(1)−N(1)	91.77(9)
Cl(2)−O(1)	1.374(3)	N(3)−Rh(1)−Cl(1)	172.75(7)
Cl(2)−O(2)	1.417(4)	N(2)−Rh(1)−Cl(1)	88.98(7)
Cl(2)−O(3)	1.419(4)	N(4)−Rh(1)−Cl(1)	94.73(6)
		N(1)−Rh(1)−Cl(1)	90.00(6)

[a] L^1 = 14-aneN_4.

ecules, related through the inversion center, are present in a triclinic cell. The slightly distorted octahedral geometry confirms that the hydride ligand is stereochemically active and occupies a regular coordination site. The hydrogen atom is positioned cis to a chlorine atom. The rhodium is displaced slightly (0.0183 Å) toward the nitrogen atom located trans to the hydride. The estimated Rh−H distance is 1.52(4) Å. Of course, as a reviewer pointed out, the Rh−H distances determined by X-ray diffraction are inherently less precise than those obtained by neutron diffraction and the true Rh−H bond could be up to 0.1−0.2 Å longer than the value given above. On the basis of the statistics, however, the reported standard deviation of 0.04 Å is correct.

The Rh−N(1) bond distance (2.197(2) Å, Table 2) is considerably longer than the remaining Rh−N bonds (average 2.066 Å), in keeping with the strong trans influence of the hydride ligand. Similarly, the Rh−N bonds trans to the hydride in the closely related $(NH_3)_5RhH^{2+}$ (2.244 Å)[14] and in *anti*-$L_2Rh_2(H)_2(\mu\text{-}H_2)](PF_6)_2$ (2.276 Å, L = 1,4,7-trimethyl-1,4,7-triazacyclononane)[15] are also much longer than the cis Rh−N bonds (2.071 and 2.082 Å, respectively). The Cl−O bond lengths in the counteranion ClO_4^- are not equal, suggesting that two of the oxygen atoms participate in hydrogen bonding with the NH protons of the cyclam. The tendency of rhodium cyclam complexes to get involved in this type of hydrogen bonding has been discussed earlier.[18]

H/D Exchange in *trans*-$L^1(D_2O)RhH^{2+}$. At pH above 7, the hydride signal in *trans*-$L^1(D_2O)RhH^{2+}$ (δ −23.5 ppm) disappears in a pH dependent process, as illustrated in Figure 2. On the same time scale, the shape and intensity of the characteristic Rh−hydride peak in the UV spectrum at 287 nm remain unchanged. Clearly, the metal hydride is not decomposing but rather engages in a H/D exchange process. The kinetics were determined in the pD range 7.95−9.12. Outside this range the kinetics were either too slow to monitor (pD < 7.95) or too fast for our mixing technique (pD > 9.12).

The plots of the NMR signal intensity against time were exponential for most of the conditions and were treated by use of the first-order rate expression. Only at pD < 8.4, the traces exhibited a minor initial phase that was faster than the rest of the reaction. Data from those experiments were fitted to an expression for biexponential kinetics, and the rate constant for the dominant, slower stage was used in further treatment. We were unable to trace the origin of the faster reaction, but note that the solutions are extremely air-

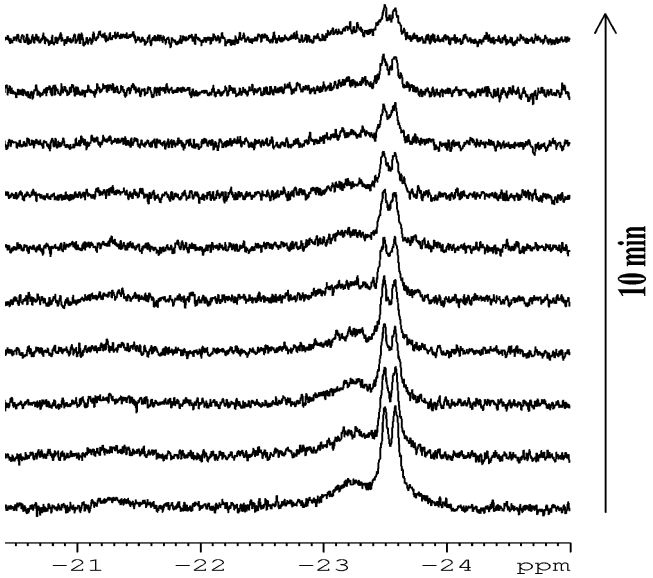

Figure 2. Disappearance of the hydride peak in *trans*-$L^1(D_2O)RhH^{2+}$ as a result of H/D exchange in D_2O at pD 8.96 and 25 °C. Spectra collected over the first 10 min of reaction are displayed.

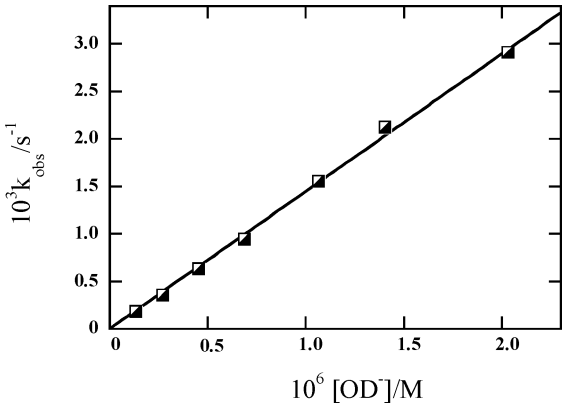

Figure 3. Plot of k_{obsd} versus [OD^-] for H/D exchange in *trans*-$L^1(D_2O)$-RhH^{2+} at 25 °C and 0.1 M ionic strength.

sensitive under the conditions of these experiments. If the slow diffusion of O_2 into the NMR tube is a problem, then this would show up at lower pH, where the reaction is slow, as observed.

The plot of the pseudo-first-order rate constants against [OD^-], Figure 3, is linear with a zero intercept, establishing a mixed second-order rate law of eq 3. The slope of the line in Figure 3 yields $k_{ex} = (1.45 \pm 0.02) \times 10^3\ M^{-1}\ s^{-1}$.

$$-d[\textit{trans}\text{-}L^1(D_2O)RhH^{2+}]/dt = k_{ex}[\textit{trans}\text{-}L^1(D_2O)RhH^{2+}][OD^-] \quad (3)$$

On the basis of the rate law, we propose a nucleophilic attack by OD^- at the hydride to form a transient Rh(I) species, $L^1(D_2O)Rh^+$, as a key step in the mechanism for H/D exchange, Scheme 1. In a rapid subsequent step, L^1-$(D_2O)Rh^+$ takes up a deuteron from the solvent and generates *trans*-$L^1(D_2O)RhD^{2+}$. The reverse of the first step is negligible under our conditions (>99% D), such that the intermediate Rh(I) engages in the productive exchange step >99% of the time.

Scheme 1

$$trans\text{-}L^1(D_2O)RhH^{2+} + OD^- \rightleftarrows trans\text{-}L^1(D_2O)Rh^+ + HOD$$

$$trans\text{-}L^1(D_2O)Rh^+ + D_2O \rightleftarrows trans\text{-}L^1(D_2O)RhD^{2+} + OD^-$$

Other mechanisms encountered in the literature on hydride exchange, such as protonation to yield a η^1-H_2 complex,[38,39] or a reaction with the solvent to generate an anion-stabilized dihydride[40] are ruled out by the stability of *trans*-$L^1(D_2O)$-RhH^{2+} in acidic solutions and by the kinetic dependence of the exchange reaction on $[OD^-]$.

To the best of our knowledge, this is the first reported example of a base-catalyzed H/D exchange involving a transition metal hydrogen bond, although a similar mechanism has been proposed for H/D exchange in *cis*-$Co(en)_2X_2^{n+}$ ($X^- = CN^-$, NO_2^-, etc.)[41] and some other complexes[42−44] involving protons on the coordinated ligands.

The substitution of D_2O in $L^1(D_2O)RhH^{2+}$ with ligands such as SCN^-, CN^-, and acetonitrile caused the rates of H/D exchange to decrease, but the precise kinetics were not determined. In an earlier study of hydrogen exchange at Ir(III), the more shielded hydride also exchanged more rapidly.[22]

SCN^- Substitution into *cis*- and *trans*-$L^1(H_2O)RhH^{2+}$ by Spectrophotometry. The absorbance/concentration data for reaction 1 were fitted to eq 4, where $\Delta\epsilon$ represents the molar absorptivity difference between the equilibrated solutions and pure *cis*/*trans*-$L^1(H_2O)RhH^{2+}$, $\Delta\epsilon_0$ is the molar absorptivity difference between *cis*/*trans*-$L^1(SCN)RhH^+$ and *cis*/*trans*-$L^1(H_2O)RhH^{2+}$, and $[SCN^-]_{eq}$ is the concentration of SCN^- in the equilibrated solutions.

$$\Delta\epsilon = \frac{\Delta\epsilon_0 K[SCN^-]_{eq}}{1 + K[SCN^-]_{eq}} \qquad (4)$$

The plot of $\Delta\epsilon$ vs $[SCN^-]_{eq}$ for *trans*-$L^1(H_2O)RhH^{2+}$ at pH 1 is shown in Figure 4. Similar plots at pH 1 for *cis*-L^1-$(H_2O)RhH^{2+}$ and 7.6 for *trans*-$L^1(H_2O)RhH^{2+}$ are presented in the Supporting Information, Figures S1 and S2. The equilibrium constants were first estimated by using the initial concentrations of SCN^- in eq 4. These estimates were then used to correct the values of $[SCN^-]_{eq}$, and the process was repeated until consistent values of K, $[SCN^-]_{eq}$, and $\Delta\epsilon_0$ were obtained. All the data are summarized in Table 3. The values of $\Delta\epsilon_0$ and known molar absorptivities of the rhodium hydrides at their absorption maxima were used to calculate

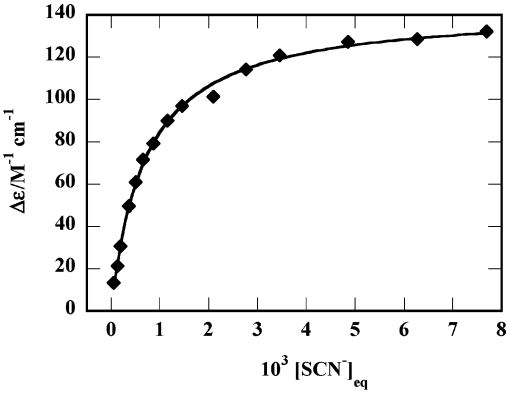

Figure 4. Plot of $\Delta\epsilon$ vs $[SCN^-]_{eq}$/M for the reaction of *trans*-$L^1(H_2O)$-RhH^{2+} (0.5−1.0 mM) with SCN^- at pH 1 and 0.2 M ionic strength ($HClO_4$ + $NaClO_4$). The solid line is the fit of experimental data to eq 4.

Table 3. Equilibrium and Absorptivity Data for the Reactions of *trans*- and *cis*-$L^1(H_2O)RhH^{2+}$ with SCN^- [a,b]

complex	$10^{-3}K/M^{-1}$	λ/nm (ϵ/M^{-1} cm^{-1})[c]
trans-$L^1(H_2O)RhH^{2+}$	1.44	287 (647)
	1.86[d]	287 (652)
cis-$L^1(H_2O)RhH^{2+}$	1.49	284 (673)

[a] L^1 = 14-aneN_4. [b] Conditions: 25 °C, pH 1, μ = 0.2 M. [c] Molar absorptivity of the product, $L^1(SCN)RhH^+$. [d] pH 7.6, μ = 0.1 M.

absolute molar absorptivities of *trans*-$L^1(SCN)RhH^+$, ϵ_{287} = 647 M^{-1} cm^{-1}, and *cis*-$L^1(SCN)RhH^+$, ϵ_{284} = 673 M^{-1} cm^{-1}. We assume, but have no experimental proof, that the thiocyanate binds to the rhodium through the "hard", nitrogen end. The UV−vis spectrum alone, in the absence of data for similar complexes, cannot identify one or the other linkage isomer reliably.

As one might have predicted, the equilibrium constants for the formation of *cis*- and *trans*-$L^1(SCN)RhH^+$ are similar. The observed rapid substitution of SCN^- for H_2O in the trans complex was also expected in view of the known kinetic trans effect of the hydride. Somewhat more surprising was the observation that the cis complex, having the water coordinated trans to a nitrogen, also reacted with SCN^- in mixing time (seconds). The NMR spectra of both cis and trans hydrides remain unchanged for prolonged periods of time under the conditions used in the equilibrium constant determination. This rules out the possibility that the cis complex had undergone isomerization to the trans form prior to the reaction with thiocyanate.

To rule out any possibility of fast thiocyanate-induced isomerization (which would be a remarkable reaction in itself), we have recorded a spectrum of an equimolar (10 mM) mixture of *cis*- and *trans*-$L^1(H_2O)RhH^{2+}$ before and after the addition of 15 mM SCN^-, Figure 5. The product mixture exhibits two hydride signals in a 1:1 integrated ratio, as expected. Another experiment used only the cis hydride. Now the product exhibited a single NMR signal (doublet) at δ −19.84, clearly showing that no *trans*-$L^1(SCN)RhH^+$ was produced.

Crystal structures of *cis*- and *trans*-$L^1(H_2O)RhH^{2+}$ are not available, but the chloro derivatives exhibit—predictably—very different Rh−Cl bond lengths, 2.549 Å (*trans*-L^1-$ClRhH^+$)[28] and 2.378 Å (*cis*-L^1ClRhH^+, see Table 2). If the

(38) Abdur-Rashid, K.; Gusev, D. G.; Lough, A. J.; Morris, R. H. *Organometallics* **2000**, *19*, 834−843.
(39) Papish, E. T.; Rix, F. C.; Spetseris, N.; Norton, J. R.; Williams, R. D. *J. Am. Chem. Soc.* **2000**, *122*, 12235−12242.
(40) Gaus, P. L.; Kao, S. C.; Darensbourg, M. Y.; Arndt, L. W. *J. Am. Chem. Soc.* **1984**, *106*, 4752−4755.
(41) Nakazawa, H.; Sakaguchi, U.; Yoneda, H.; Morimoto, Y. *Inorg. Chem.* **1981**, *20*, 973−979.
(42) Anderson, G. K.; Saum, S. E.; Cross, R. J.; Morris, S. A. *Organometallics* **1983**, *2*, 780−782.
(43) Bruce, M.; Swincer, A. G.; Thomson, B. J.; Wallis, R. C. *Aust. J. Chem.* **1980**, *33*, 2605−2613.
(44) Kimura, M.; Morita, M.; Mitani, H.; Okamoto, H.; Satake, K.; Morosawa, S. *Bull. Chem. Soc. Jpn.* **1992**, *65*, 2557−2559.

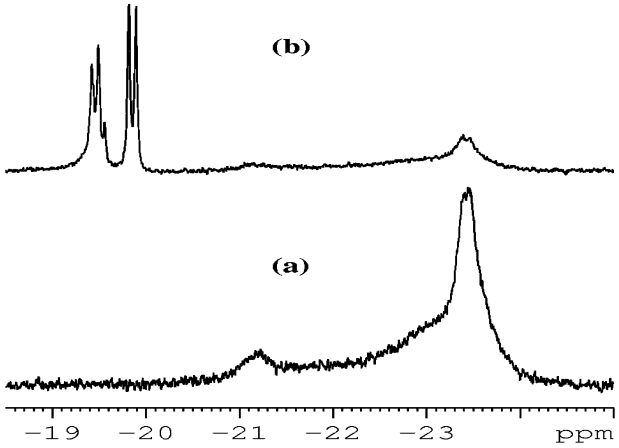

Figure 5. ^{1}H NMR spectra recorded (a) before and (b) after the addition of 15 mM SCN^- to a mixture of *cis*-$L^1(D_2O)RhH^{2+}$ (10 mM) and *trans*-$L^1(D_2O)RhH^{2+}$ (10 mM) in D_2O at pD 1 and 25 °C.

Rh−H_2O bond lengths in *cis*- and *trans*-$L^1(H_2O)RhH^{2+}$ also differ significantly, as one would expect, then clearly the shorter Rh−H_2O bond in the cis hydride does not translate into slow kinetics. It would appear that the cis configuration imposes greater strain and increased crowding at the substitution site, thus reducing the advantage of the trans influence in the other isomer. The rate constants for SCN^- substitution have not been determined, and the trans complex may well be more reactive. At this stage, our only argument is that rapid ligand substitution, as observed for *cis*-$L^1(H_2O)RhH^{2+}$, is highly unusual for an unactivated Rh(III) complex. In the next section we present data suggesting that some cis complexes may undergo substitution even faster than their trans counterparts.

Ligand Substitution in *cis*- and *trans*-$L^1(D_2O)RhH^{2+}$ by ^{1}H NMR. The hydride region of the ^{1}H NMR spectra of equilibrium product mixtures for the reactions between *trans*-$L^1(D_2O)RhH^{2+}$ and the halides Cl^-, Br^-, and I^- and for the reactions of *cis*- and *trans*-$L^1(D_2O)RhH^{2+}$ with SCN^-, CN^- and CD_3CN are depicted in Figures 6 and 7, respectively. These and subsequent experiments used much higher concentrations of rhodium hydrides (10−20 mM) than experiments utilizing spectrophotometry (submillimolar levels). The speciation under such different concentration conditions may not be the same. The more concentrated NMR solutions may, and probably do (see later), contain some dimeric forms. Also, the proportion of anion-ligated forms is much greater even when only stoichiometric amounts of anions are present.

As shown in Figure 6b, sharp signals are obtained at 2 °C. The major doublet (δ −23.3) in the bottom right panel is assigned to *trans*-$L^1(D_2O)RhH^{2+}$, but the two minor doublets were not identified. The different chemical environment for the hydride in the three species is probably created by various degrees of hydrogen bonding, ion pairing, and/or monomer/dimer equilibria. The low-intensity peak at δ −21.1 is assigned to *trans*-L^1ClRhH^+. Apparently, not all the chloride was removed by recrystallization of the crude chloro hydride from water, see Experimental Section. The sharp, intense doublets in solutions containing 0.1 M halide ions are assigned as *trans*-L^1XRhH^+ (X = Cl, Br, I). The

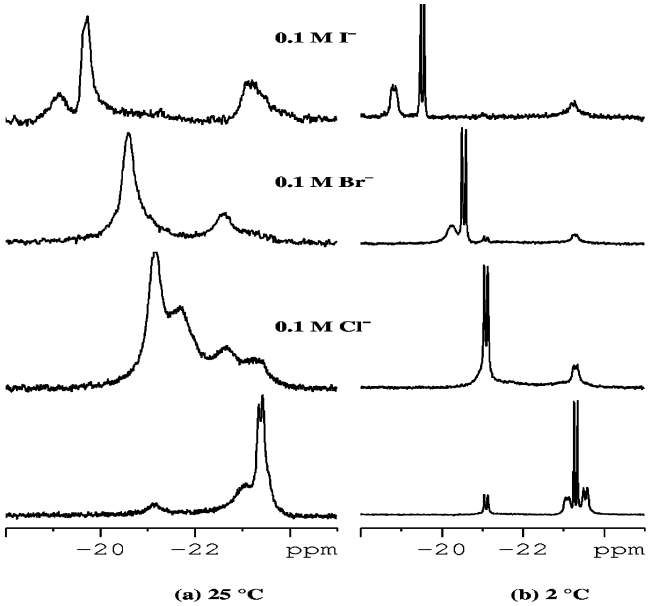

Figure 6. ^{1}H NMR spectra of the products of the reaction of *trans*-$L^1(D_2O)RhH^{2+}$ (12−20 mM) with 0.1 M X^- (X = Cl, Br, or I) in air-free D_2O at 25 °C (left panel) and 2 °C (right panel). Solutions of *trans*-$L^1(D_2O)RhH^{2+}$ in the bottom spectra contained small amounts of *trans*-L^1ClRhH^+, which appears at −21.1 ppm.

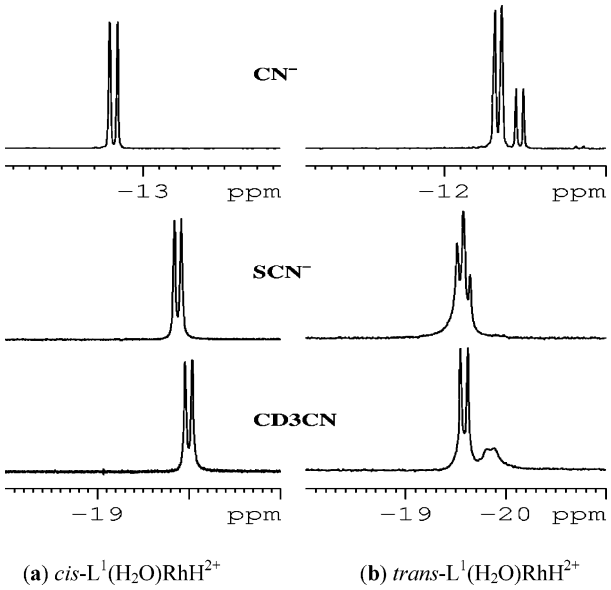

Figure 7. ^{1}H NMR spectra of the products of the reactions of (a) *cis*-$L^1(D_2O)RhH^{2+}$ and (b) *trans*-$L^1(D_2O)RhH^{2+}$ with CN^-, SCN^-, and CD_3CN at room temperature in air-free D_2O, pD 1. The two bottom spectra use the same *x*-axis.

low-intensity, broad signals on the lower-field sides could not be identified. Possibly, they correspond to small amounts of halide- or hydride-bridged dimeric species.

The broadening of the hydride peaks at 25 °C is believed to be caused by the exchange of aqua and halide ligands. The exchange may involve free anions in solution in a process that is at least in part dissociative in character, eq 5, or it can take place via a ligand-bridged transition state or intermediate, eqs 6 and 7. Both mechanisms are feasible because of the lability of the trans position. Five-coordinate d^6 species such as $Ir(H)_2(X)P_2$ (X = halide or pseudohalide,

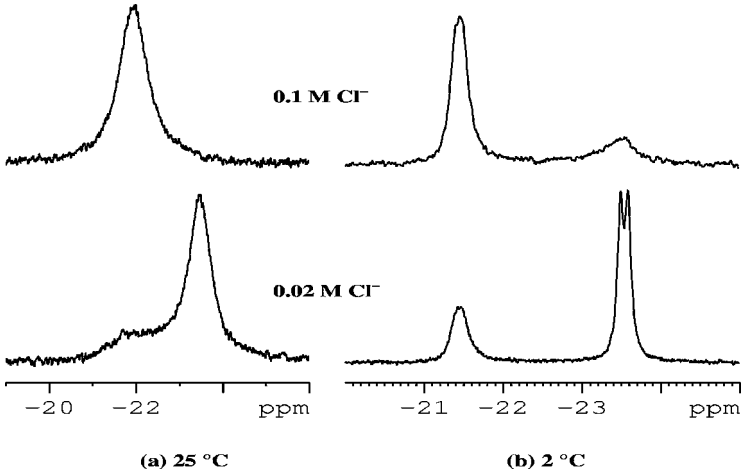

Figure 8. The hydride region ^{1}H NMR spectra for a mixture of *cis*-$L^1(D_2O)RhH^{2+}$ (20 mM) and Cl^- (0.02 and 0.1 M) in D_2O at (a) 25 °C and (b) 2 °C.

P = bulky phosphine) have been reported to undergo rapid ligand redistribution via transient halide-bridged dimers.[45]

$$L^1(D_2O)RhH^{2+} + X^- \rightleftarrows L^1XRhH^+ + D_2O \quad (5)$$

$$L^1(D_2O)RhH^{2+} + L^1X{*}RhH^+ \rightleftarrows L^1HRh{-}X{-}{*}RhL^1H^{3+} + D_2O \quad (6)$$

$$L^1HRh{-}X{-}{*}Rh{-}L^1H^{3+} \underset{-D_2O}{\overset{+D_2O}{\rightleftharpoons}} L^1XRhH^+ + L^1(D_2O){*}RhH^{2+} \quad (7)$$

To find out whether trace amounts of Rh(II), possibly present in these solutions or generated photochemically upon exposure to room light, are catalyzing ligand exchange processes, the spectra of *cis*- and *trans*-$L^1(D_2O)RhH^{2+}$ were recorded in the presence of more than a 2-fold excess of hydrogen peroxide, which is known to oxidize macrocyclic rhodium(II) complexes rapidly.[46] The spectra remained unaffected, which rules out $L^1(D_2O)Rh^{2+}$ or any other reducing impurity as a major factor in line broadening.

The ligands CN^-, SCN^-, and CD_3CN are strongly bound to Rh(III). The hydride peaks at room temperature are sharp, Figure 7, and ligand exchange is not apparent. In fact, the addition of SCN^- to a mixture of *trans*-$L^1(D_2O)RhH^{2+}$ and Cl^- at room temperature produced the same spectrum as the reaction between *trans*-$L^1(D_2O)RhH^{2+}$ and SCN^- in the absence of added chloride, demonstrating the much greater affinity of rhodium hydride for SCN^-.

In both types of experiments, multiple species were observed. The same is true for solutions of *trans*-$L^1(D_2O)$-RhH^{2+} containing CN^- or acetonitrile-d_3. For example, the spectrum shown at the bottom right in Figure 7b (CD_3CN) was resolved into three sharp doublets upon cooling of the solution to 2 °C (Supporting Information, Figure S3). All the spectra were fully reproducible and remained unchanged even after repeated recrystallizations of *trans*-$[L^1(H_2O)RhH]$-$(ClO_4)_2$, clearly showing that impurities were not the problem. Moreover, the starting material, *trans*-$[L^1ClRhH]$-Cl, exhibits only one doublet in DMSO-d_6 at −20.34 ppm, as expected for a single geometrical isomer.[28] As mentioned earlier, the complex spectra of the trans complexes in D_2O solutions in Figures 6 and 7 must reflect the presence of several species in solution equilibria involving ligand exchange, hydrogen bonding, and ion pairing. Such processes have a major effect on NMR spectra in nonaqueous solutions,[47−50] but there are no comparable data in water that would allow us to draw parallels with our work. Surprisingly, the NMR spectra of the cis complexes are much simpler, as shown in the left-hand panel of Figure 7, although the cis complexes are expected to be involved in similar types of solution equilibria.

The hydride resonances in *cis*- and *trans*-$L^1(CN)RhH^+$ (Figure 7, top spectra) show a dramatic downfield shift, in agreement with literature precedents.[51] Coordination of π-acceptor ligands CO, PMe_3, and ethylene trans to a hydride in iridium(III) complexes also causes a pronounced downfield shift of the hydride resonances.[26]

A comparison of the NMR spectra in Figures 6 and 8 suggests that the water−chloride exchange in *cis*-$L^1(D_2O)$-RhH^{2+} (Figure 8) may be even faster than for the trans isomer. As can be seen in Figure 8b (top spectrum), cooling of the solution to 2 °C did not stop the exchange at either chloride concentration. The signal at δ −21.4 ppm is broad as opposed to the sharp doublet at −21.1 ppm (Figure 6b, second spectrum from bottom) obtained for *trans*-$L^1(D_2O)$-RhH^{2+} in the presence of 0.1 M Cl^-. Possibly, the chloride-bridged dimeric species of the cis complex are more labile because of the nonbonding interactions which cause a rapid decay to the monomeric forms and thus accelerate the exchange. The broad doublet at δ −23.5 in Figure 8b (bottom spectrum) is assigned to *cis*-$L^1(D_2O)RhH^{2+}$. As can be seen, the exchange process is observed even at low concentrations

(45) Poulton, J. T.; Hauger, B. E.; Kuhlman, R. L.; Caulton, K. G. *Inorg. Chem.* **1994**, *33*, 3325−3330.
(46) Bakac, A. *Inorg. Chem.* **1998**, *37*, 3548−3552.
(47) Crabtree, R. H. In *Modern Coordination Chemistry. The Legacy of Joseph Chatt*; Leigh, G. J., Winterton, N., Eds.; Royal Society of Chemistry: Cambridge, U.K., 2002; pp 31−44.
(48) Limbach, H. H. *Magn. Reson. Chem.* **2001**, *39*, S1−S2.
(49) Reich, H. J.; Borst, J. P.; Dykstra, R. R.; Green, D. P. *J. Am. Chem. Soc.* **1993**, *115*, 8728−8741.
(50) Epstein, L. M.; Shubina, E. S. *Coord. Chem. Rev.* **2002**, *231*, 165−181.
(51) Whitesides, G. M.; Maglio, G. *J. Am. Chem. Soc.* **1969**, *91*, 4980−4986.

of chloride, where *cis*-$L^1(D_2O)RhH^{2+}$ is the predominant species at both temperatures.

Acknowledgment. This research was supported by the U.S. Department of Energy, Office of Basic Energy Sciences, Division of Chemical Sciences, under Contract W-7405-ENG-82 with Iowa State University of Science and Technology. We are grateful to the Roy J. Carver Charitable Trust, which provided funds to initiate this project. We also thank Mr. Eric Leblanc for help with some experiments, and the reviewers for helpful comments.

Supporting Information Available: Listings of bond lengths and angles, atomic coordinates, and anisotropic displacement parameters, CIF, plots of equilibrium data, and an NMR spectrum. This material is available free of charge via the Internet at http://pubs.acs.org.

IC034130V